THE AIR FLOW AROUND AN ISOLATED MOUNTAIN

Kouji Izumi
Ricoh Co., Ltd. R&D Center, Yokohama, Japan
Yousay Hayashi
National Inst. of Agro-Environmental
Sciences, Ibaraki, Japan

International Symposium
on Scale Modeling

July 18-22, 1988
Tokyo

The Japan Society of Mechanical Engineers

THE AIR FLOW AROUND AN ISOLATED MOUNTAIN

Kouji Izumi
Ricoh Co., Ltd. R&D Center, Yokohama, Japan
Yousay Hayashi
National Inst. of Agro-Environmental
Sciences, Ibaraki, Japan

ABSTRACT

The airflow over Mt. Fuji was simulated by use of a model cone which moves in the water tank with a constant speed. The structure of the flow field depends upon Reynolds number and tip angle of the model cone.

A horse-shoe vortex was formed at the upstream surface of the cone. And the separated region appeared over the downstream surface of the cone. The shape of the separated flow area is a triangular quadrant. The existence of a high shear zone along the climbing trails, in the leeside of Mt. Fuji, was supported by the present experimental results.

INTRODUCTION

In order to investigate the air flow properties around an isolated mountain, some water tank experiments were carried out using a single cone modeled after the shape of Mt. Fuji. It has been pointed out in the previous analysis that the distribution of surface wind direction, around Mt. Fuji, is almost the same as the flow pattern over an model obstacle (Soma, 1969; Sato and Onda, 1974). Especially during the winter season, a strong westerly wind prevails over Mt. Fuji which is located in the central part of Japan. Therefore the flow field will closely resemble the conditions in a water tank experiment.

To understand the actual distribution of wind direction over Mt. Fuji, flag-shaped trees were used in the present study. This kind of tree has been recognized as a good indicator of surface wind conditions. A distribution map showing occurence points of accidental falls was also prepared to explain the appearance of a separation area on the leeside of the mountain surface.

DISTRIBUTION OF SURFACE WIND USING FLAG-SHAPED TREES

Flag-shaped trees are formed by the prevailing winds. Fig.1 shows a typical tree (Larix Kaemferi) at a point, 2300 m heigh, on the northern slope of Mt. Fuji. Although the physiological processes have not yet been made clear, the effects of wind on a tree's growth can be seen in the respective regions of the world ranging from the tropics to the polar regions and from the coasts to the alpine zones of the mountains (Yoshino, 1973). Using an inverse relationship, the authers made an investigation of wind direction by means of flag-shaped trees widely distributed around Mt. Fuji. The surveyed trees were Larix Kaemferi, Abies Mariesii, Tsuga diversifolia and so on.

Fig. 1 Typical flag-shaped tree on the northern slope of Mt. Fuji.

Fig.2 shows the distribution of the dominant flow direction deduced from flag-shaped trees. On the foot of the west side of the mountain, the flow direction is almost oriented to the north. At the north and south points of the mountain, the winds are turned aside in the same direction as the component of the slope. On the mountain's leeside, as shown by arrows over the south-southeast part, the flow direction returns to the north with the component of the south wind. The results mentioned above are generally well suported by the previous investigation by Oka (1972).

Around Mt. Fuji, the timberline is located almost on the contour line at 2400 m heigh and 1400 m heigh at the west and at the east side of the

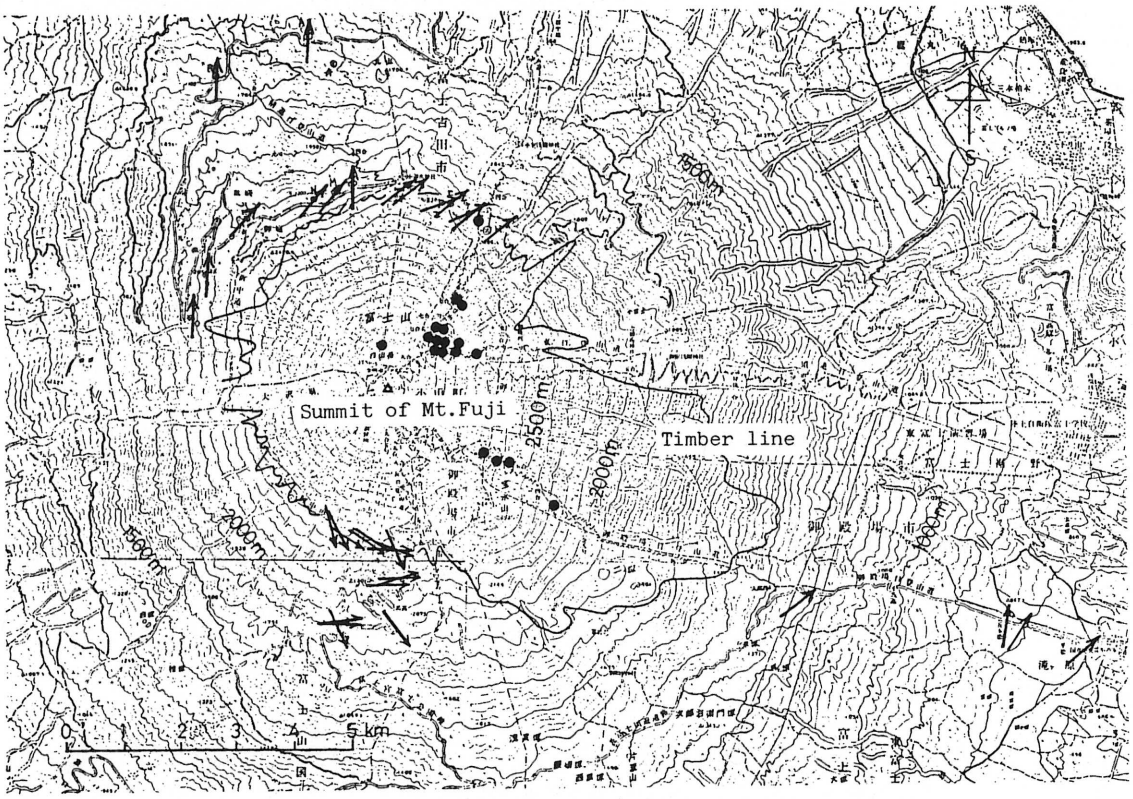

Fig. 2 Distribution map of the flow direction deduced from flag-shaped trees. Arrows mean the flow direction, ● the accident points by strong wind, ▲ the summit of Mt. Fuji and solod line the timber line.

mountain respectively. This is also represented in Fig.2. This line coincides with the lower margin of debris area caused by the eruption of Mt. Fuji. At the southeast part of the mountain there are no trees. Unfortunately we can not find a roundabout flow pattern at the backside of the mountain.

OCCURENCE OF MOUNTAINEER'S DISASTERS

During a 12 year period (from 1964 to 1975), a mountaineer's disaster occurred 86 times on Mt. Fuji (Hayashi and Izumi, 1978). The monthly change of frequency of the occurence is shown in Fig.3. There are two peaks, one in July and one in November. The peak in July is mainly due to injury by falling stones, and November's peak is due to accidental sliding caused by gusty winds.

The year by year variation of the number of disasters is tabulated in Table 1. About 28% (24 times) of the whole were classified as the accidents caused by gusts or strong winds and the distribution is represented in Fig.2. The accidents occured at the southeast and the northeast sides of the slope above 2000 m. These areas are empirically named by mountain climbers as "Tsumuji zone" or "Gust zone" because of the severeness of the wind.

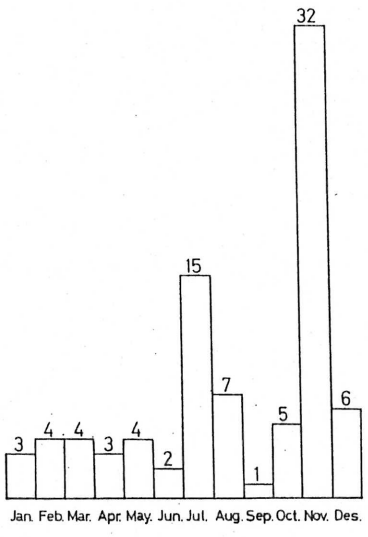

Fig. 3 Monthly variation of mountaineer's disaster (1964 - 1975).

EXPERIMENTAL APPARATUS AND METHOD

Model experiments were carried out using a water tank located at Research & Institute Applied Mechanics, Kyusyu University, which has a test section of 45 cm wide, 40 cm deep and 600 cm long.

A cone on a flat plate moves with a constant velocity through the length of the tank (Fig. 4). The cone's velocity is adjusted from 0.6 cm/sec to 4 cm/sec in the water tank. The models used for the experiment were made of brass, with a tip angle

Table 1 Year by year change of the number of mountaineer's disasters (1964 - 1975).

	Winter Season	'64	'65	'66	'67	'68	'69	'70	'71	'72	'73	'74	'75	Total
CAUSE	Gust or Strong W.	-	5	3	-	3	4	1	2	3	1	2	-	24
	Snowstorm	-	2	1	-	1	1	-	-	-	-	-	-	5
	Abalanche	-	-	-	-	-	-	-	1	-	-	-	-	1
	Thunder-bolt	-	-	-	-	-	-	-	-	1	-	-	-	1
	Fog	-	1	-	-	-	-	-	-	-	-	1	-	2
	Others	-	9	4	-	2	-	1	-	1	-	2	1	20
	Unknown	1	5	7	5	3	1	3	-	1	2	4	1	33
Total		1	22	15	5	9	6	5	3	6	3	9	2	86

of θ = 30°, 90° and 120° respectively. The diameter of each cone's base was 3 cm. Particularly in the case of θ = 120°, we used a model with a cone diameter of 9 cm.

The dimensions of the base plate were 24 cm wide, 40 cm long and 1 cm thick. In order to prevent the flow separation from the leading edge of this plate, the plate was inclined on a 1% grade. The position of the cone's center is fixed from the leading edge of the plate by a distance of 9 cm.

The Reynolds number Re, based on the diameter of the cone D, was 200 - 1200. An electrolytic precipitation method was adopted for flow visualization.

RESULT OF THE EXPERIMENT

(1) Flow Fields in the Case of θ = 90°

Fig. 5 shows the flow fields around the cone on a flat plate with θ = 90°. The structure of the flow field depends upon the Reynolds number and the tip angle of the cone. In Fig. 5 and 6, a series of left hand side flow fields were observed in the top view and right hand flow field were observed in the side view. The flow direction of a uniform flow is from left to right.

A white dye indicates the integrated streak sheet. The "integrated streak sheet", first introduced by Taneda (1978), is composed of all the fluid particles which have emerged from the total surface of the cone's body.

In Fig. 5, Reynolds numbers based on the diameters of the cone base are 200, 400, 600, 800, 1000 and 1200 respectively. At a low Reynolds number, Re = 200, the separated region appeared over the downstream surface of the cone. The shape of the separated region on the surface of the cone is a triangular quadrant. At the separated region of the wake, a pair of trailing vortices can be observed.

Regarding the rotation of the trailing vortices, it can be shown that the right side and left side vortex rotates in a clockwise and a counter-clockwise direction respectively. The origination of trailing vortices is at the surface of the cone and they continue side by side.

The phenomena of interference between a pair of trailing vortices were generated by the condition of a high Reynolds number, such as Re = 400. Subsequently, vortices in a half ring shape were shed from the cone successively in increments of the Re value. At the same time, the separation

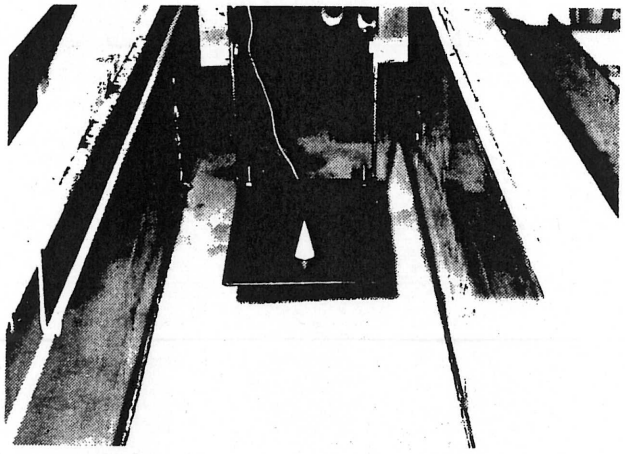

Fig. 4 A model cone on a flat plate in the water tank.

lines oscillated periodically over the leeside of the cone. Furthermore, the shedding periodicity of the vortex was interrupted at Reynolds numbers above Re = 1000.

In these photographs, the flow pattern at the upstream surface of the cone and the plate is not clear, but a horse-shoe vortex was formed at that area for every Reynolds number.

(2) Flow Pattern in the Case of θ = 120°

Fig. 6 shows the flow patterns with θ = 120°. Fundamentally, the flow patterns are similar to the case of θ = 90°. Below a Reynolds number of 600, a pair of trailing vortices are formed in the wake. Above a Reynolds number of 800, interference between a pair of trailing vortices occured. At a higher Reynolds number, it will be seen that vortices in a half ring shape are shed periodically. Each shedding vortex is linked to the next by a vortex, in a half ring shape establishing a continuous chain. Compared to the case of θ = 90°, the periodicity of vortex shedding in the case of θ = 120° is in uniform intervals.

The shedding frequency f (Hz) of the vortex is a function of the Reynolds number and the diameter of the cone base D. The following relation is available:

$$f = 0.43 \left(U / D \right).$$

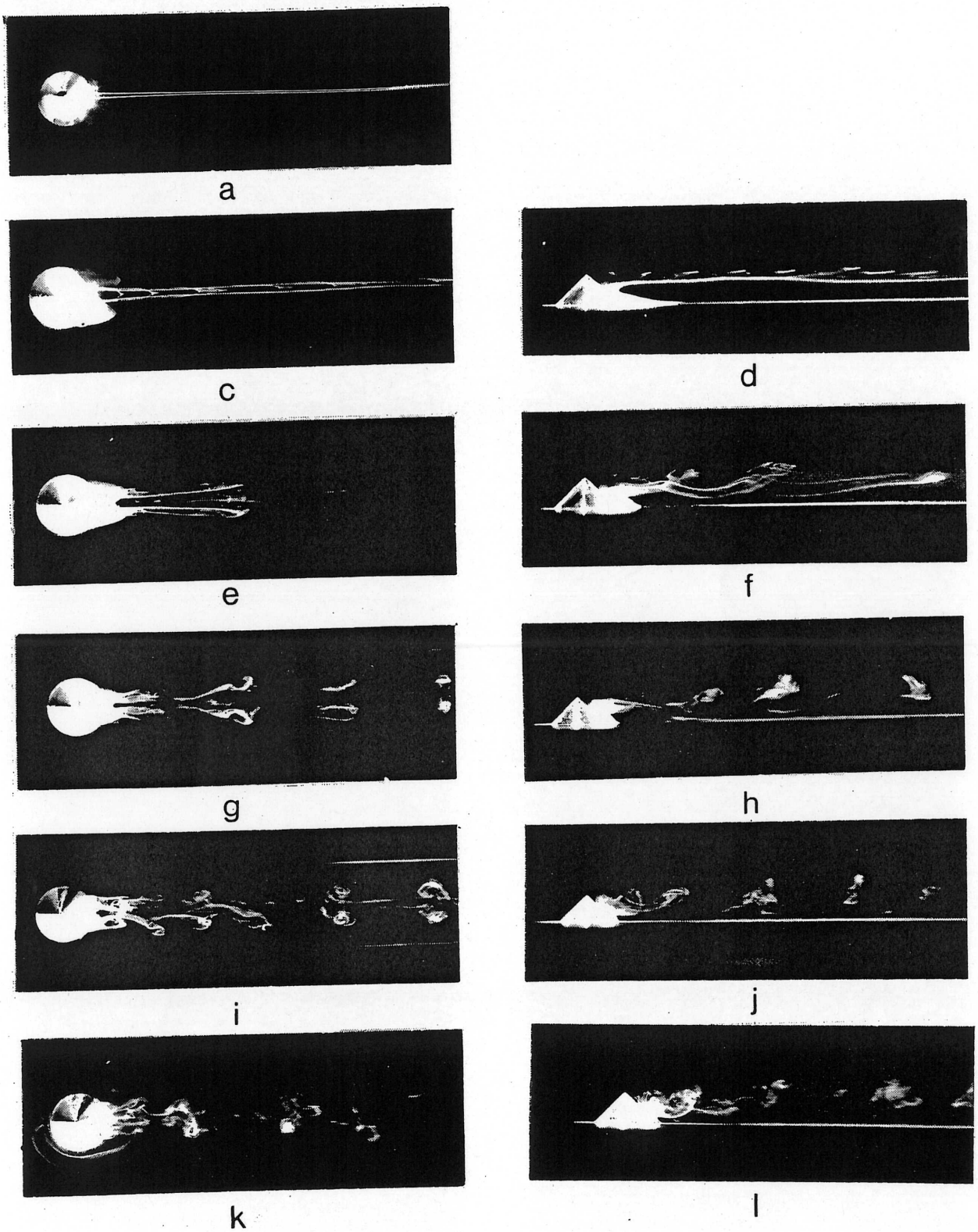

Fig. 5 Flow fields around a cone with $\theta = 90°$.

(a):Re=200, (c) (d):Re=400, (e) (f):Re=600, (g) (h):Re=800,
(i) (j):Re=1000, (k) (l):Re=1200
(a),(c),(e),(g),(i),(k) are plain views and (d),(f),(h),(j),
(l) are side views.

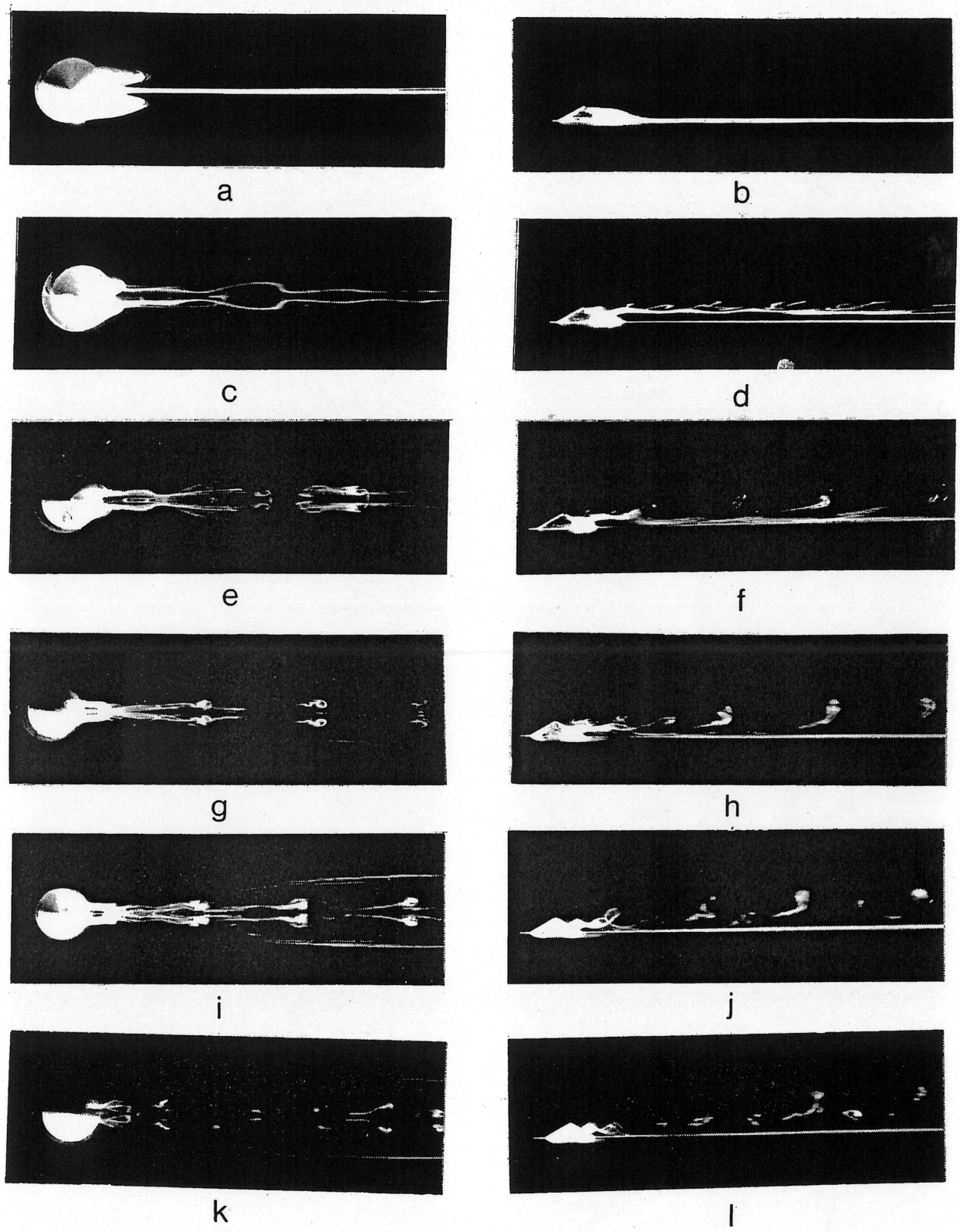

Fig. 6 Flow fields around a cone with θ = 120°.

(a) (b):Re=600, (c) (d):Re=800, (e) (f):Re=1000, (g) (h):Re=1200,
(i) (j):Re=1400, (k) (l):Re=1600
(a),(c),(e),(g),(i),(k) are plain views and (b),(d),(f),(h),(j),
(l) are side views.

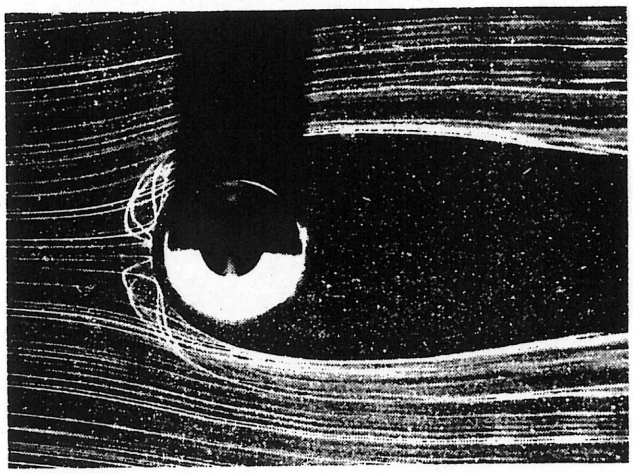

Fig. 7 Streak lines in the case of θ = 30° and Re = 300.

Here U is the velocity of the uniform flow. For every Reynolds number, the shape of the separated region on the surface of the cone is a triangular quadrant. The tip angle of the triangular quadrant depends upon the Reynolds number. When the Reynolds number increased, the angle of the quadrant decreased gradually.

(3) Horse-Shoe Vortex

For every cone's tip angle and Reynolds number, that was evaluated, a horse-shoe vortex was definitely formed at the upstream surface of the cone and the plate.

Fig. 7 shows streak lines on the flat plate around the cone in the case of θ = 30°, Re = 300. A solder wire which has diameter of 0.3 mm, was positioned in front of the cone. The distance between the wire and the cone's center was 7 cm and the height of the wire from the plate was 0.5 cm. This solder wire was used for the electrolytic precipitation method.

It will be clearly demonstrated that the streak lines roll up at the upstream surface of the cone. The streak line indicates the existence of a horse-shoe vortex.

(4) Schematic Bird'f Eye View of the Flow Field

Fig. 8 and 9 represent the schematic flow field

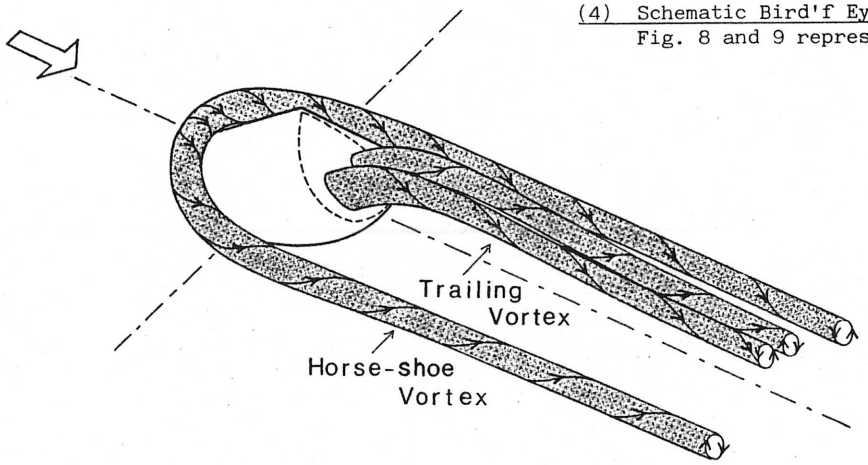

Fig. 8 Schematic flow field with a horse-shoe vortex and trailing vortex at a low Reynolds number.

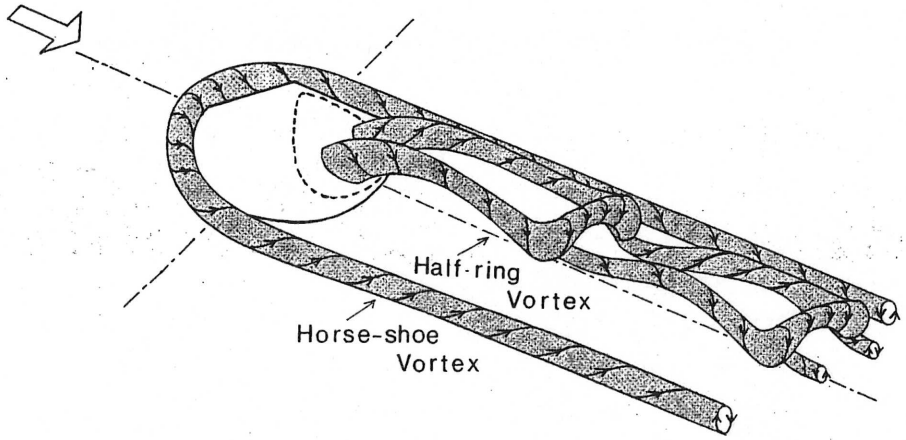

Fig. 9 Schematic flow field with oscillation motion at a heigh Reynolds number.

in the case of $\theta = 120°$. It has already been mentioned above that the flow field depends upon the Reynolds number. At a low Reynolds number, the flow field consists of a horse-shoe vortex and a pair of trailing vortices as shown in Fig. 8. At a higher Reynolds number, the flow fields in particular on the leeside region of the model, begin to oscillate. The wake consists of a horse-shoe vortex and shedding vortices in a half ring shapes, establishing a continuous chain as seen in Fig. 9.

(5) Surface Flow Pattern in the Case of $\theta = 120°$

In order to compare the distribution of the surface flow of Mt. Fuji, using flag-shaped trees and the experimental results, the surface flow on a cone is investigated. Fig. 10 shows the stream line on the cone's surface using the electorolytic corrosion method and the electrolytic precipitation method.

Fig. 11 shows the schematic traces of the stream lines and the direction of flow. In these figures, a stagnation point (A) is observed on the upstrem surface of the cone. In the upstream area, away from the stagnation point, the white dye oozed out onto the surface of the flat plate. In this area, the direction of the surface is contrary to the direction of the uniform flow. This pattern indicates the existence of a horse-shoe vortex.

On the other hand, the separation area in the shape of a triangular quardrant is observed on the leeward surface of the cone. In Fig. 11, the broken line (p/ indicates the separation line. In this separation area, it is clearly seen that this is the origination point (E1) (E2) for a pair of trailing vortices.

Furthermore, in this separated area, the flow direction on the cone's surface compares with the direction of the climbing trails on the slope. Consequently, flow layers with intense vorticity separate from the sepatation line in this area.

DISCUSSION

The surface distribution of accidental falls caused by strong gusts forms the straight lines of a triangular quardrant as seen in Fig. 2. The separation line, as seen from the experimental results using the water tank, reveals the same shape as in Fig. 11. To our surprise, the locus of mountain climbing trails is in approximately straight lines forming a triangular quardrant as in Fig. 2.

It is well known that a high shear layer of the flow exists near the separation line of the flow. Also, the existence of a high shear layer means the organization of strong gusts. Consequently, we can easily imagine that the mountaineers who climb the mountain trails in the winter season have placed themselves in a very dangerous situation.

CONCLUSION AND REMARKS

In order to elucidate the relationship between the flow field around Mt. Fuji and the surface distribution of the mountaineer's accidental falls, model flow experiments around the cone on a flat plate were carried out using a water tank. The flow fields depend upon the Reynolds number and are classified into two types which can be seen when the tip angle $\theta = 120°$. On the leeward surface of the cone, the shape of the flow separated area is a triangular quadrant.

By way of comparison, the surface distribution

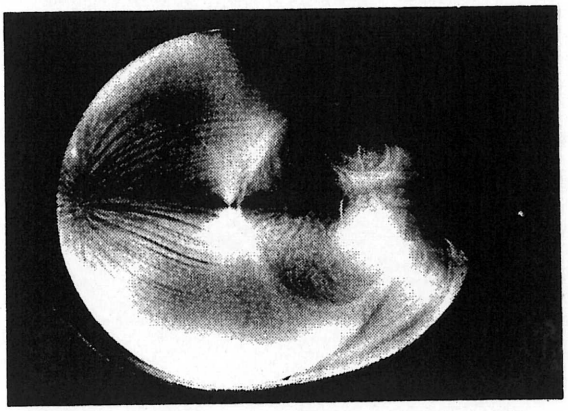

Fig. 10 Stream line on the model cone.

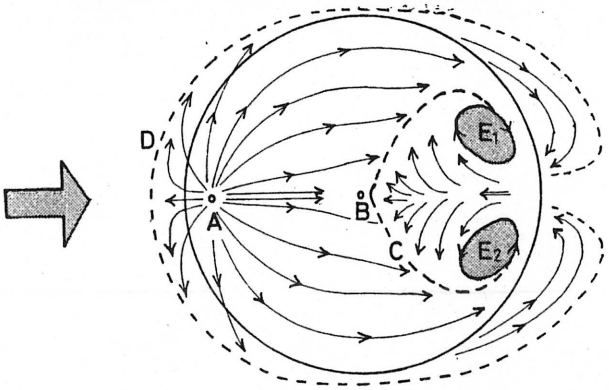

Fig. 11 Schematic trace of Fig. 11.

A: Stagnation point, B: Tip of the model, C: Separation line on the model, D: Separation line on the plate, E1 and E2: Eddy

of the occurrence of mountaineer's accidental falls caused by strong gusts, mainly in the winter season forms the straight lines of a triangular quadrant. The visualized features of the separation line mentioned above were also strongly related to the distribution of these accidents.

A similarity could be shown by the experimental results and natural phenomena data.

Finally, we notice that the location of mountain climbing trails approximates with the outline of the separation line of the flow. We don't know who decided the location of the mountain climbing trails or how the decision was made. We wonder if the relationship between these facts can make Mt. Fuji a dangerous climb for mountaineers in the winter season.

ACKNOWLEDGEMENT

The authors would like to express their sincere thanks to Professor S. Taneda and Professor M. Inokuchi for their valuable advice and encouragements. Thanks are also due to Mr. M. Sato and Mr. S. Bolema for their much appreciated support.

REFERENCES

1. Hayashi, Y. and Izumi, K., Bull. Envirn. Res. Cen., Univ. of Tsukuba, Vol. 2, pp. 97-102, 1978.
2. Oka, S., Geogr. Rep., Tokyo Metroporitan Univ., Vol. 6, pp. 15-29, 1972.
3. Sato, H. and Onda, Y., Kisyo Kenkyu Note, MSJ, No. 118, pp. 55-64, 1974.
4. Soma, S., Pap. Met. Geoph., Vol. 20, pp. 11-74, 1969.
5. Taneda, S., Bull. Res. Inst. Appl. Mech., Kyushu Univ., Vol. 47, 1978.
6. Yoshino, M.M., Clim. Notes, Univ. of Tsukuba, Vol. 12, pp. 1-52, 1973.